Bone 94 (2017) 10–21

Contents lists available at ScienceDirect

Bone

journal homepage: www.elsevier.com/locate/bone

Full Length Article

Inhibition of BET proteins and epigenetic signaling as a potential treatment for osteoporosis

Marc Baud'huin [a,b,c,1], François Lamoureux [a,b,1], Camille Jacques [a,b], Lidia Rodriguez Calleja [a,b], Thibaut Quillard [a,b], Céline Charrier [a,b], Jérome Amiaud [a,b], Martine Berreur [a,b], Bénédicte Brounais-LeRoyer [a,b], Robert Owen [d], Gwendolen C. Reilly [d], James E. Bradner [e,f], Dominique Heymann [a,b,c], Benjamin Ory, PhDAssociate Professor [a,b,*]

[a] INSERM, UMR 957, équipe labellisée ligue 2012, 1 Rue Gaston Veil, 44035 Nantes, France
[b] Physiopathologie de la Résorption Osseuse et Thérapie des Tumeurs Osseuses Primitives, Université de Nantes, Nantes Atlantique Universités, EA3822, 1 Rue Gaston Veil, 44035 Nantes, France
[c] Nantes University Hospital, Nantes, France
[d] Department of Materials Science and Engineering, INSIGNEO Institute for In Silico Medicine, University of Sheffield, Sheffield, UK
[e] Department of Medical Oncology, Dana-Farber Cancer Institute, Harvard Medical School, 44 Binney Street, Boston, MA 02115, USA
[f] Department of Medicine, Harvard Medical School, 25 Shattuck Street, Boston, MA 02115, USA

ARTICLE INFO

Article history:
Received 7 March 2016
Revised 7 September 2016
Accepted 22 September 2016
Available online 23 September 2016

Keywords:
Osteoporosis
Epigenetic
Bromodomain
Inhibitor
Osteoblast
Osteoclast

ABSTRACT

Histone modifications are important for maintaining the transcription program. BET proteins, an important class of "histone reading proteins", have recently been described as essential in bone biology. This study presents the therapeutic opportunity of BET protein inhibition in osteoporosis. We find that the pharmacological BET protein inhibitor JQ1 rescues pathologic bone loss in a post-ovariectomy osteoporosis model by increasing the trabecular bone volume and restoring mechanical properties. The BET protein inhibition suppresses osteoclast differentiation and activity as well as the osteoblastogenesis *in vitro*. Moreover, we show that treated non-resorbing osteoclasts could still activate osteoblast differentiation. In addition, specific inhibition of BRD4 using RNA interference inhibits osteoclast differentiation but strongly activates osteoblast mineralization activity. Mechanistically, JQ1 inhibits expression of the master osteoclast transcription factor NFATc1 and the transcription factor of osteoblast Runx2. These findings strongly support that targeting epigenetic chromatin regulators such as BET proteins may offer a promising alternative for the treatment of bone-related disorders such as osteoporosis.

1. Introduction

Bone is a dynamic tissue in constant change through a physiological remodeling process involving bone-specific cells; the osteoclasts which are responsible for the resorption of old or damaged bone and the osteoblasts which are specialized in the formation of a new bone [1,2]. In physiological conditions the balance between bone resorption and bone formation is required to maintain constant bone mass for the majority of adulthood. Disruption of this physiological balance leads to the development of bone-related disorders. Osteoporosis is the most prevalent bone disease in older women and men, characterized by a low bone mass, reduced bone mineral density, and deterioration of bone microarchitecture leading to an increased fracture risk. In osteoporosis the rate of bone resorption exceeds the rate of bone formation, thus decreasing the bone mass [1]. Currently, most available agents in clinical use to treat osteoporosis inhibit bone resorption, whereas only a few stimulate bone formation and restore bone mass [3].

Recent molecular and genetic studies, identifying numerous local and systemic regulators of bone resorption, have considerably improved our molecular knowledge of bone remodeling [4]. Amongst them, epigenetic regulation which include posttranslational histone modifications, miRNA-mediated post-transcriptional regulation and DNA methylation play an important role in bone biology [5,6].

Bromodomain and extra-terminal domain (BET) protein family (BRD2, BRD3, BRD4, and BRDT), through its ability to bind to acetylated lysine on histone tails, is an important class of "histone reading protein" [7]. Bromodomains act as a scaffold for molecular complexes at the recognized histone sites in order to regulate chromatin accessibility to transcription factors and RNA polymerase [8]. Recently, several BET

* Corresponding author at: INSERM, UMR-957, 1 Rue Gaston Veil, 44035 Nantes, France.
E-mail address: Benjamin.ory@univ-nantes.fr (B. Ory).
[1] These two authors contributed equally to the work.

http://dx.doi.org/10.1016/j.bone.2016.09.020
8756-3282/

protein inhibitors have been developed including JQ1 and I-BET151. They were described as a new therapeutic approach in various preclinical cancer models [9–13]. In addition, these small-molecule inhibitors of BET proteins were recently identified to suppress bone destruction in many distinct inflammatory diseases (arthritis, periodontitis, bone tumour, osteoporosis) [11,14–16].

In this study, we confirm the therapeutic potential of BET protein inhibition, by using JQ1, to reverse bone loss induced by estrogen deficiency. Moreover, our findings deeply demonstrate that JQ1 rescues bone mass and bone strength in ovariectomy-induced osteoporotic mice by interfering with osteoblast and osteoclast differentiation. We observed that JQ1 treated-osteoclasts could still activate osteoblastogenesis *in vitro*. Importantly, we provide evidence that BET protein inhibition does not affect the structure and mechanical properties of bone in physiological conditions. These findings reinforce the therapeutic potential of BET protein inhibition in diseases characterized by an impairment of bone formation.

2. Materials and methods

2.1. Therapeutic agents

The BRD4 inhibitor, JQ1, was kindly provided by James Bradner (Dana-Farber Cancer Institute) and used for *in vitro* and *in vivo* studies. This synthetic compound selectively targets the acetyl-lysine binding pocket of BET proteins. For the *in vitro* studies, JQ1 was dissolved in dimethyl sulfoxide (DMSO) at 10 mM stock solution and stored at −20 °C. For the *in vivo* studies, JQ1 was dissolved in DMSO at 50 mg/ml, and then diluted in 10% hydroxypropyl beta cyclodextrin (HP-β-CD, Sigma Aldrich) to obtain the final concentration, 50 mg/kg, and stored at 4 °C. The 10% HP-β-CD was prepared in sterile water, which was filtered with 0.22 μm filter.

2.2. Animal treatment

All procedures involving mice [their housing in the Experimental Therapeutic Unit at the Faculty of Medicine of Nantes (France) and care, the method by which they were anesthetized and killed, and all experimental protocols] were all conducted in accordance with the institutional guidelines and were approved by the "Ethic Committee for Animal Experimentation" (CEEA.PdL. Licence: 2011.32). 8-week old C57BL/6 female mice ovariectomized (OVX) or SHAM-operated (SHAM) from Janvier Labs (Le Genest-Saint-Isle, France), were left untreated for 2 weeks, and then treated with JQ1 (50 mg/kg) or vehicle ($n = 6$ for each group), twice a day by intraperitoneal (I.P.) injection. In a second experiment, 6-week old C57BL/6 male mice (Janvier labs) were treated with JQ1 (50 mg/kg) or vehicle twice a day by I.P. injection ($n = 6$ for each group). For dynamic bone histomorphometry, mice were injected (I.P.) with calcein (20 mg/kg) at 7 days and 2 days before sacrifice. At sacrifice, the femurs, tibiae and vertebrae L4 were collected for further analysis.

2.3. Micro computed tomography (microCT) analysis

Micro computed tomography (microCT) analysis was performed as previously described [3]. Briefly, tibias were scanned using high-resolution microcomputed tomography (Skyscan 1076, Kontich, Belgium) at 50 kV and 200 μA using a 0.5 mm aluminium filter and a detection pixel size of 9 μm. Images were captured every 0.7° through 180° rotation, and analysed using Skyscan software. Trabecular structures positioned 0.2 mm below the growth plate, were quantified over a length of 1 mm. Cortical bone positioned 1 mm below the growth plate, was quantified over a length of 1 mm. For the lumbar vertebra L4, the central 60% of the trabecular bone was analysed. Bone volume/total volume fraction (BV/TV), trabecular thickness (Tb.Th.), trabecular separation (Tb.Sp.), trabecular number (Tb.N.) and cortical thickness (Ct. Th) were determined.

2.4. Bone histomorphometric analysis

Tibias were decalcified with 4.13% EDTA and 0.2% paraformaldehyde in phosphate buffered saline (PBS) for 96 h using the KOS microwave histostation (Milestone, Kalamazoo, MI) before embedding in paraffin. Sections (3 μm thick, Leica Microsystems) were analysed by tartrate-resistant acid phosphatase (TRAP) staining as described previously [17,18]. Immunostaining for Osterix was performed as described [17] with a rabbit anti-osterix antibody (1/25; Abcam, Cambridge, MA, http://www.abcam.com). Quantification of osteoclast number ($TRAP^+$ cells) and osteoblast number ($osterix^+$ cells) in the metaphyseal spongiosa was evaluated manually using ImageJ software in 0.4 mm^2 region of interest (ROI). For undecalcified histology, tibias were methylmethacrylate-embedded for microtome sectioning (6 μm) for von Kossa staining.

For the dynamic histomorphometry, tibia were dissected and embedded in methylmethacrylate as previously described [3]. Thin sections were mounted unstained and analysed using an image analysis software program (Qwin) interfaced with a microscopy using a DMRXA epifluorescent microscope (Leica). All comparisons of staining intensities were made at 200× magnifications.

2.5. Three point bending

Bones were subjected to three point bending analysis using a Bose Electroforce 3200 mechanical testing machine with a 450 N load cell. Rounded supports and press head were used with a constant span support distance of 6 mm for all femurs. Bones were positioned horizontally with the press head contacting the midshaft. A preload of 0.25 N was applied to the bone before compressing at a constant force of 0.25 N/s until failure. From the force-displacement curve, stiffness (N/mm) was calculated from the linear region and maximum load from the peak force.

2.6. Osteoclast differentiation

Generation of osteoclasts from human $CD14^+$ monocytes was described previously [19]. Briefly, purified $CD14^+$ cells from different donors were cultured in α-MEM with 10% FCS and 25 ng/ml human M-CSF (R&D systems). After 4 days of culture, 100 ng/ml RANKL was added. Multinucleated cells formed with 3 nuclei and more were counted after TRAP staining (Sigma, France). The resorption capacity was assessed on 96-well Corning Osteo Assay ®. Mature osteoclasts were cultured with 25 ng/ml hMCSF, 100 ng/ml RANKL and JQ1 at various concentrations. After 3 days of culture, cells were removed with bleach solution and resorption pits area was quantified using Image J software (NIH, Bethesda, MD).

2.7. Osteoblast differentiation

Before passage 5, human MSCs were seeded at 10^4 cells per centimeter square in 96-well plates in DMEM supplemented with vitamin D3 (10^{-8} M; Hoffmann-La Roche, Basel, Switzerland), dexamethasone (10^{-8} M; Sigma) and with or without JQ1 as indicated (this represented day 0 for MSC osteogenic differentiation). Three days later, freshly prepared ascorbic acid (50 μg/ml; Sigma) and β-glycerophosphate (10 mM; Sigma) was added to allow mineralization, this medium being changed every 2–3 days. Alizarin red-S staining was used to detect the mineralized nodules formed *in vitro* as described previously [20]. Briefly, between days 19 and 21, cells were fixed in ice-cold 70% ethanol for 1 h and incubated with Alizarin red-S (40 mM, pH 7.4; Sigma) for 10 min at room temperature. After extensive washing, images were captured using a stereo microscope (Stemi 2000-C; Zeiss,

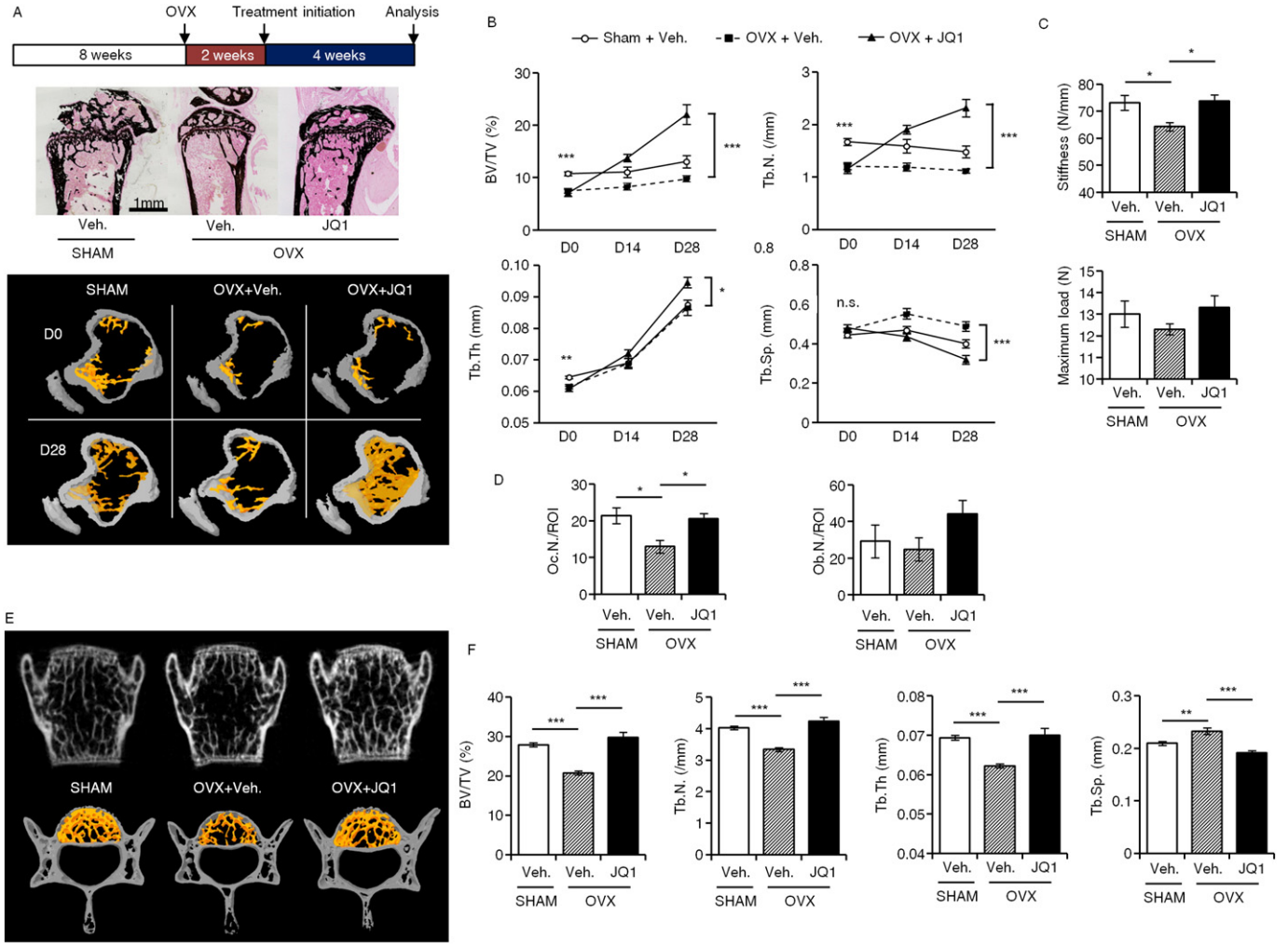

Fig. 1. JQ1 rescues osteoporosis in ovariectomized mice. (A) Representative longitudinal sections coloured with Von Kossa staining and representative transverse microCT images of the proximal tibia metaphysis, taken *ex vivo*, from SHAM mice treated with vehicle or OVX mice treated with vehicle or JQ1 for 28 days ($n = 6$ for each group) (B) MicroCT analysis of trabecular bone volume (BV/TV (%)), trabecular number (Tb.N (/mm), trabecular thickness (Tb.Th (mm)) and trabecular separation (Tb.Sp (mm)) of the tibia of SHAM mice treated with vehicle or OVX mice treated with vehicle or JQ1. (C) Three point bending analysis of stiffness and maximum load of the left femur of SHAM mice treated with vehicle (open bars) or OVX mice treated with vehicle (hatched bars) or JQ1 (black bars). ($n = 4$ for each group). (D) Histogram showing osteoclast number (Oc.N./ROI) and osteoblast number (Ob.N./ROI) in SHAM mice treated with vehicle (open bars) or OVX mice treated with vehicle (hatched bars) or JQ1 (black bars) at the end of experiment (28 days). (E) Representative longitudinal and transverse microCT images of lumbar vertebra L4, taken *ex vivo*, from SHAM mice treated with vehicle or OVX mice treated with vehicle or JQ1 for 7 days. (F) MicroCT analysis of trabecular bone volume (BV/TV (%)), trabecular number (Tb.N (/mm)), trabecular thickness (Tb.Th (mm)) and trabecular separation (Tb.Sp (mm)) of lumbar vertebra L4 of SHAM mice treated with vehicle (open bars) or OVX mice treated with vehicle (hatched bars) or JQ1 (black bars). ROI is a region of interest of 0.4 mm^2 Data represent mean ± SEM, $^{*}p < 0.05$, $^{**}p < 0.01$, $^{***}p < 0.001$, compared to vehicle by ANOVA followed by a post test (Bonferroni).

Oberkochen, Germany), and mineralized surfaces were quantified using the Qwin software (Leica, Nussloch, Germany).

2.8. Quantitative reverse transcription-PCR

Total RNA was extracted from cultured cells using TRIreagent (Invitrogen Life Technologies). Total RNA was reversed transcribed using the ThermoScript RT-PCR System (Life Technologies). Real-time monitoring of PCR amplification of complementary DNA (cDNA) was performed using DNA primers (primers sequences are available upon request) on CFX96 real-time PCR detector system (Bio-Rad, Marnes la Coquette, France) with SYBR PCR Master Mix buffer (Bio-Rad). Target gene expression was normalized to GAPDH levels in respective samples as an internal standard, and the comparative cycle threshold (Ct) method was used to calculated relative quantification of target mRNAs. Primers for each gene are

Fig. 2. BET proteins inhibition inhibits osteoclast differentiation. Purified human CD14+ monocytes were cultured for 7 days in the presence of M-CSF and RANKL. (A) mRNA levels of hNFATc1, hBRD2, hBRD3 and hBRD4 were assessed by qRT-PCR at different time points of the culture (D4, D5 and D7). Results are expressed as fold change compared to the condition without RANKL at day 4. (B) Purified human CD14+ monocytes were cultured for 7 days in the presence of M-CSF, RANKL and JQ1 at different concentrations. TRAP colouration was performed at the end of the culture period (scale bar, 100 mm) and multinucleated TRAP-positive cells were counted under a light microscope (coloured bars) and the cell viability was assessed by Crystal Violet (line) (results are expressed as percentage of the control condition without JQ1). (C) Resorption lacunae and percentage of resorbed area obtained by osteoclasts (from CD14+) cultured on OsteoAssay plate treated with or without JQ1. Digital images were captured using resident image capture, NIH ImageJ software was used for image analysis. (D) Purified human CD14+ monocytes were cultured for 7 days in the presence of M-CSF, RANKL and JQ1 as indicated. mRNA levels of *hTRAP*, *hCtsk*, *hNFATc1* and *hMMP9* were assessed by qRT-PCR at the end of the culture period. Data represent mean ± SEM, $^{*}p < 0.05$, $^{**}p < 0.01$, $^{***}p < 0.001$, compared to vehicle by ANOVA followed by a post test (Bonferroni). (For interpretation of the references to colour in this figure legend, the reader is referred to the web version of this article.)

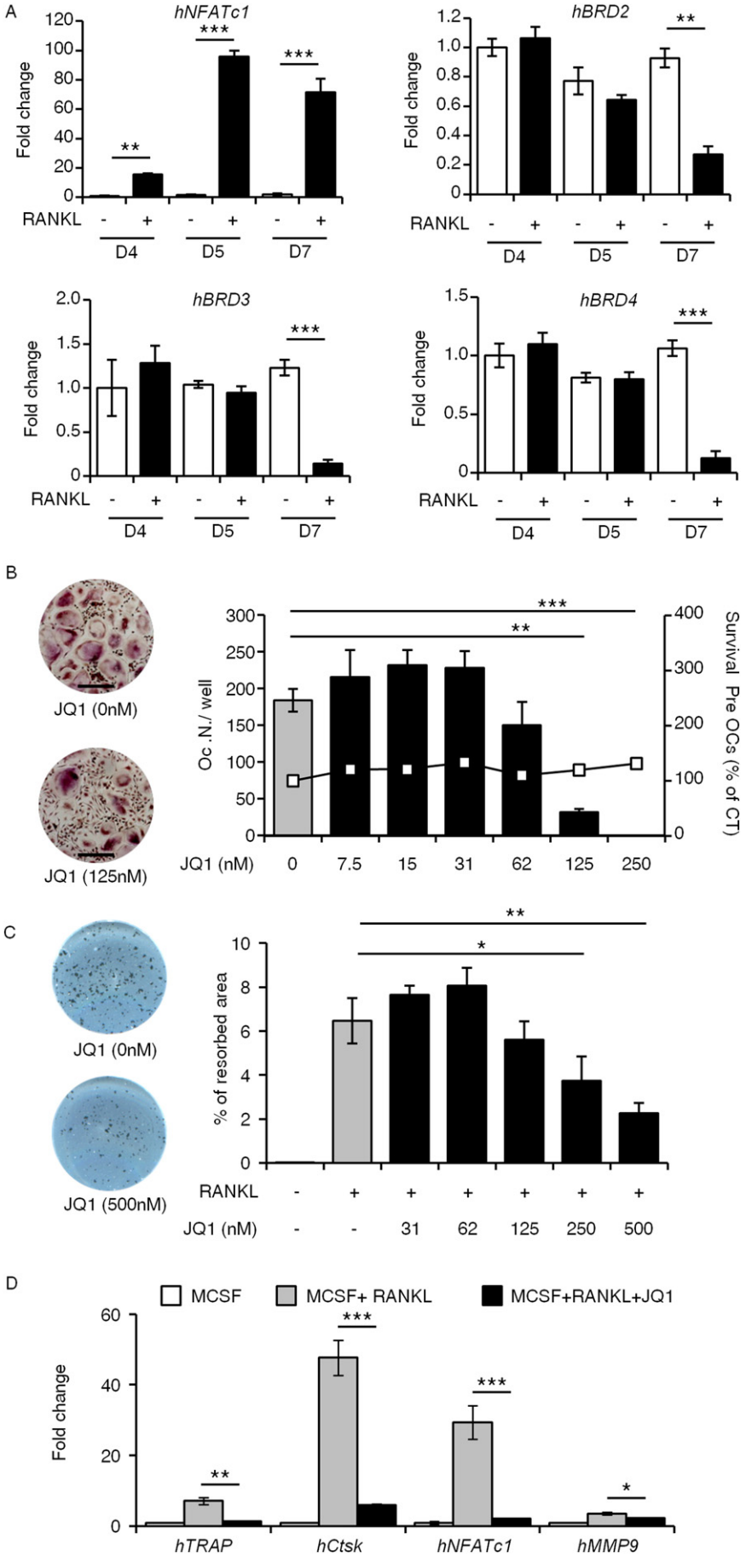
A
hNFATc1
hBRD2
hBRD3
hBRD4
Fold change
RANKL
D4
D5
D7
B
JQ1 (0nM)
JQ1 (125nM)
Oc.N./ well
Survival Pre OCs (% of CT)
JQ1 (nM) 0 7.5 15 31 62 125 250
C
JQ1 (0nM)
JQ1 (500nM)
% of resorbed area
RANKL
JQ1 (nM) 0 31 62 125 250 500
D
MCSF
MCSF+ RANKL
MCSF+RANKL+JQ1
hTRAP
hCtsk
hNFATc1
hMMP9

described in Supplemental Information. Each assay was performed in triplicate.

2.9. Gene silencing

Knock-down of *BRD2*, *BRD3*, and *BRD4* using short hairpin RNA (shRNA) in human pre-OCs and human MSCs cells were obtained by lentiviral cell transduction as described previously [21]. They were used for lentivirus production following the protocols provided with the ViraPower Lentiviral Expression System (Invitrogen). A multiplicity of infection of 10 was used to transduce MSCs cells and of 4 was used to transduce pre-OCs cells. shRNA targeting LacZ was used as a control.

2.10. Statistical analysis

Data were tested for normality using a Kolmogorov-Smirnov test. The mean ± SEM was calculated for all groups and compared by two-tailed paired Students *t*-test or by ANOVA, with the Dunnett's multiple comparisons test for *post-hoc* analysis. $p < 0.05$ was used as the criteria for statistical significance.

3. Results

3.1. BET protein inhibition rescues osteoporosis in ovariectomized mice

We first examined whether a BET protein inhibitor, JQ1, could increase bone mass in ovariectomized mice with established bone loss. We left SHAM-operated or ovariectomized (OVX) 8-week-old mice without treatment for 2 weeks to notice a significant bone loss, then treated them with vehicle or JQ1 (50 mg/kg twice per day) for 4 weeks (Fig. 1A). Von Kossa stained cross sections and micro-computed tomography (μCT) analysis of the metaphyseal region of the proximal tibia confirmed the expected trabecular bone loss caused by ovariectomy (34% of trabecular bone volume decrease compared with SHAM, $p < 0.001$) before treatment (Fig. 1A and fig. 1B). After 4 weeks of JQ1 treatment, trabecular bone volume was higher than in OVX mice treated with vehicle (125%, $p < 0.001$) and SHAM-operated controls (68%, $p < 0.01$; Fig. 1B). The increase in trabecular bone volume was associated with greater trabecular number and trabecular thickness (respectively +106%, $p < 0.001$ and +9%, $p < 0.05$) and lower trabecular separation (−34%, $p < 0.001$; Fig. 1B). Three-point bending of the left femoral diaphysis was performed to test bone strength. Ovariectomy without treatment resulted in lower stiffness (−14.3%, $p < 0.05$, Fig. 1C) and maximum load (−5.4%) compared to SHAM-operated control mice. JQ1 treatment of OVX mice resulted in greater bone strength, with a higher stiffness (17.7%, $p < 0.05$, Fig. 1C) and maximum load (8.3%) compared to OVX-vehicle mice. Histomorphometric analysis of trabecular bone in the proximal tibia at the end of the experiment, showed a decrease in osteoclast and osteoblast number in OVX animals treated with vehicle (Oc.N./ROI and Ob.N/ROI; Fig. 1D) while a treatment with BET protein inhibitor significantly increased osteoclast and osteoblast number suggesting a greater bone remodeling. Similarly to tibiae, trabecular bone mass in the lumbar vertebra L4 was significantly greater in OVX-JQ1 treated mice compared to OVX mice treated with the vehicle after 7 days of treatment (Fig. 1E and F). These results demonstrate that JQ1 treatment strongly reverses an established osteopenia induced by ovariectomy.

3.2. BET protein inhibition blocks osteoclast differentiation and activity

To understand the mechanisms responsible for the correction of osteopenia in OVX mice, we examined the effects of BET protein inhibition on OB and OC differentiation. The mRNA expression levels of the different BET proteins were quantified along with osteoclast differentiation. This revealed a late decrease of *BRD2*, *BRD3* and *BRD4* expression associated to an increase of the master transcription factor of osteoclastogenesis *NFATc1* (Nuclear factor of activated T-cells cytoplasmic 1 under the activation of NF-κB pathway [22]) at day 7 (Fig. 2A), suggesting that BET proteins are required in the first steps of osteoclast formation. To evaluate the importance of the BET proteins during osteoclast differentiation we first assessed the effect of JQ1 on osteoclast differentiation. JQ1 significantly inhibited osteoclastogenesis in a dose dependent manner without affecting survival, as revealed by OC precursor viability measured by Crystal Violet staining (Fig. 2B). Moreover, JQ1 treatment significantly reduced the osteoclastic bone resorption *in vitro* (43% decrease of resorbed surface at 250 nM, Fig. 2C). This inhibition of osteoclast formation and activity came with a strong reduction of tartrate-resistant acid phosphatase (*TRAP*, 80%) and cathepsinK (*Ctsk*, 87%) expression, two markers of OC differentiation and activity (Fig. 2D).

To identify the underlying mechanism of JQ1-mediated inhibition of OC differentiation, we then tested the activity of NF-κB using a luciferase-based reporter construct containing its consensus-binding site. Cells expressing RANK were transfected with the NF-κB promoter construct and were then treated with RANKL or TNFα in the presence or absence of JQ1. Our results showed that the inhibition of BET proteins by JQ1 treatment reduced RANKL- and TNFα-stimulated NF-κB transcriptional activity (respectively >30% and 40%, Supplementary Figure S1). These findings are sustained by the decrease of NF-κB target genes *NFATc1* and *MMP9* mRNA expression (respectively 92% and 34%, Fig. 2D) in JQ1-treated OC precursors. Our findings demonstrate that inhibition of BET proteins disrupt both OC formation and activity.

3.3. Specific inhibition of BRD2, BRD3 and BRD4 recapitulate JQ1 inhibition of osteoclast differentiation in vitro

To make sure the inhibition of the BET proteins was the key mechanism behind the observed effect of JQ1 on osteoclastogenesis, we transduced pre OCs ($CD14^+$ cells) with a combination of shBRD2, shBRD3 and shBRD4 (shBRDs). The knock-down of *BRD2*, *BRD3*, and *BRD4* were validated at mRNA levels 2 days after transduction (Fig. 3A). The efficiency of three different shRNA for the BRDs was previously validated on human mesenchymal stem cells (hMSCs) (Supplementary Figure S2).

Transduced pre OCs were then cultured with RANKL to induce their differentiation. After 7 days of culture in differentiation medium, shBRDs-transduced cells did not differentiate into OCs while pre-OCs transduced with shLacZ were still able to differentiate into OCs. It is associated with a reduction of relative expression of h*NFATc1* and h*MMP9* (respectively 90% and 66%, Fig. 3B). This confirmed that the simultaneous inhibition of the three BRDs recapitulates the effects of JQ1 on osteoclastogenesis.

Pre OCs were then transduced with shRNAs specific for BRD2 or BRD3 or BRD4. In these conditions, we observed the same effects that we previously described with a combination of three shBRDs. The silencing of BRD2, BRD3 or BRD4 led to a decrease in osteoclast formation (respectively 95%, 90% and 92%) and to an inhibition of *NFATc1* and *MMP9* expression levels (Fig. 3C), confirming the critical role of each BRDs in osteoclastogenesis.

3.4. BET protein inhibition decreases osteoblast differentiation in vitro

The effects of BET protein inhibition on osteoblastic differentiation have been tested using JQ1 inhibitor. Human MSCs from different donors were cultured for 21 days in the presence of OB differentiation medium. The expression levels of the different BET proteins were evaluated throughout OB differentiation *in vitro* and revealed a concomitant late increase of *BRD2*, *BRD3* and *BRD4* parallel to the late stage marker of osteoblastogenesis alkaline phosphatase (*ALP*), at days 14 and 21 (Fig. 4A).

In order to evaluate the importance of the BET proteins during OB differentiation, we set up two different experiments. First, hMSCs were cultured for 21 days in presence of OB differentiation medium and JQ1 continuously for 21 days. Alizarin red Staining was performed at the end of the culture to assess mineralization and therefore OB

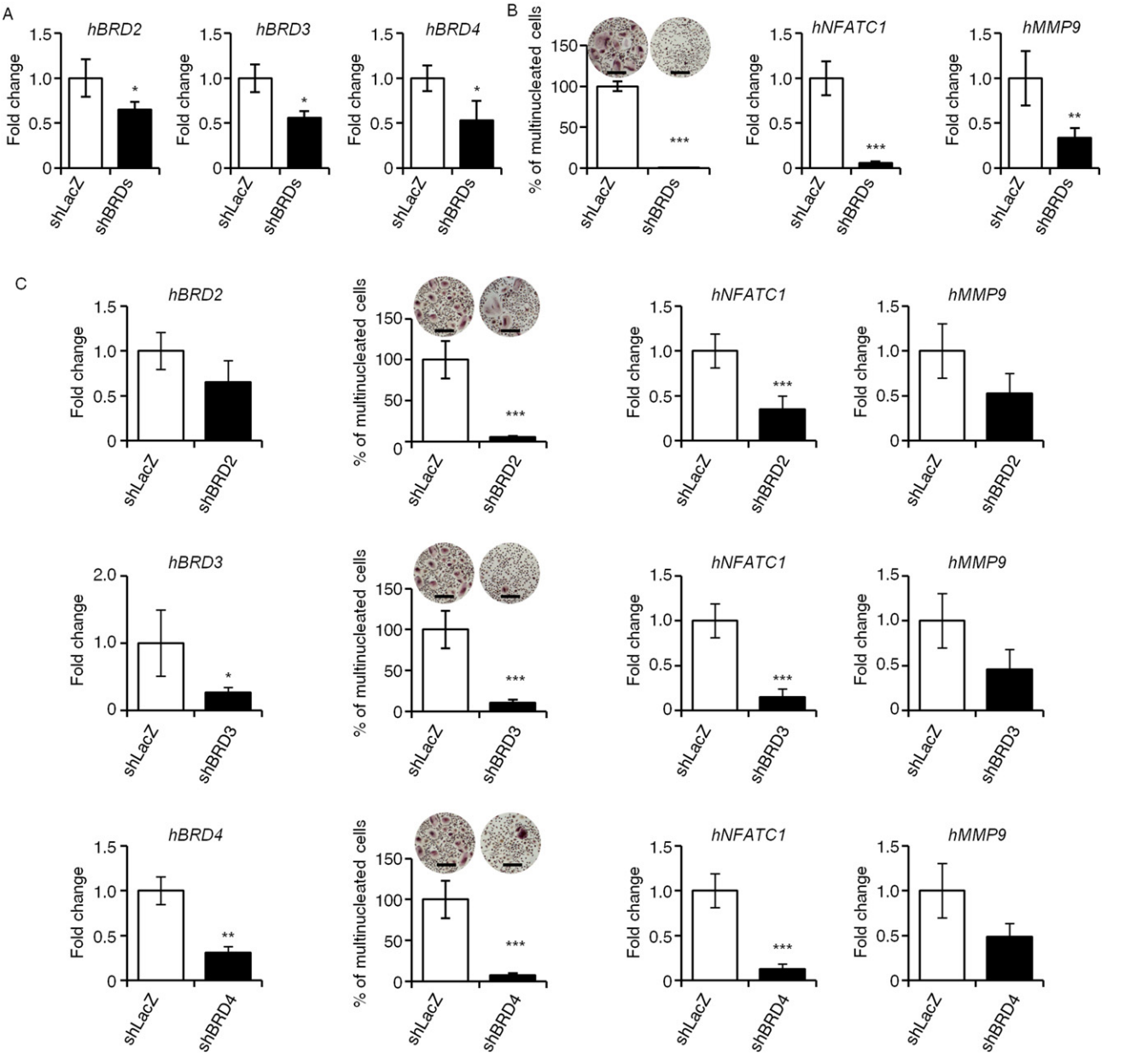

Fig. 3. Inhibition of BRD2, BRD3 and BRD4 recapitulate JQ1 inhibition of osteoclast differentiation *in vitro*. (A) Human CD14 + cells were transduced with a combination of shBRD2, shBRD3, shBRD4 (shBRDs). After 48 h, h*BRD2*, h*BRD3* and h*BRD4* RNA levels were assessed by qRT-PCR. (B) After 7 days, cultured in OC differentiation medium, multinucleated TRAP-positive cells were counted under a light microscope (scale bars, 100 mm) and expression of h*NFATc1* and h*MMP9* were assessed by qRT-PCR. (C) Human CD14 + cells were transduced with shBRD2 or shBRD3 or shBRD4. After 48 h, expression of *hBRD2*, *hBRD3* and *hBRD4* RNA levels were respectively assessed by qRT-PCR. After 7 days, cultured in OC differentiation medium, multinucleated TRAP-positive cells were counted under a light microscope and expression of *hNFATc1* and *hMMP9* were assessed by qRT-PCR. The control condition shLacZ is common to the experiments with shBrd2, shBRD3 and shBRD4 in panel C. The same picture has been taken to illustrate the experiments. Data represent mean ± SEM, $^{*}p < 0.05$, $^{**}p < 0.01$, $^{***}p < 0.001$ compared to vehicle by Student *t*-test.

differentiation (Fig. 4B). JQ1 treatment (125 nM) resulted in a marked decrease of mineralization without any effect on cell proliferation/survival as revealed by cell viability assessed by Crystal Violet staining (Fig. 4B). We then examined the expression of a critical transcription factor for OB differentiation, *RUNX2*, and a late stage marker of osteoblastogenesis, *ALP*. In both cases, JQ1 treatment led to a significant decrease of their gene expression (Fig. 4B).

Second, to evaluate when the expression of the BET proteins is the most critical to OB differentiation, the same experiments were repeated with a JQ1 treatment only applied during the last 7 days of the differentiation protocol. Similar effects to the first experiment were observed in terms of inhibition of mineralization and *RUNX2* and *ALP* expression (Fig. 4C). As suggested by Fig. 4A, the BET proteins expression in the last steps of the OB differentiation is of utmost importance.

Considering the resulting increase in bone mass in OVX-mice treated with JQ1 and the direct effects of JQ1 observed on osteoblasts and osteoclasts, we next asked whether JQ1 could interfere into the osteoclast-osteoblast crosstalks and promote bone formation. We investigated *in vitro* the activity of preosteoclasts (pre OCs) and osteoclasts (OCs) treated with JQ1 on the differentiation of mesenchymal stem cells into osteoblasts. We revealed that in both case, JQ1 did not modify the ability of pre OCs and OCs to activate osteoblastogenesis as suggested by the expression of *hRunx2* (Fig. 4D and Supplementary Figure S3).

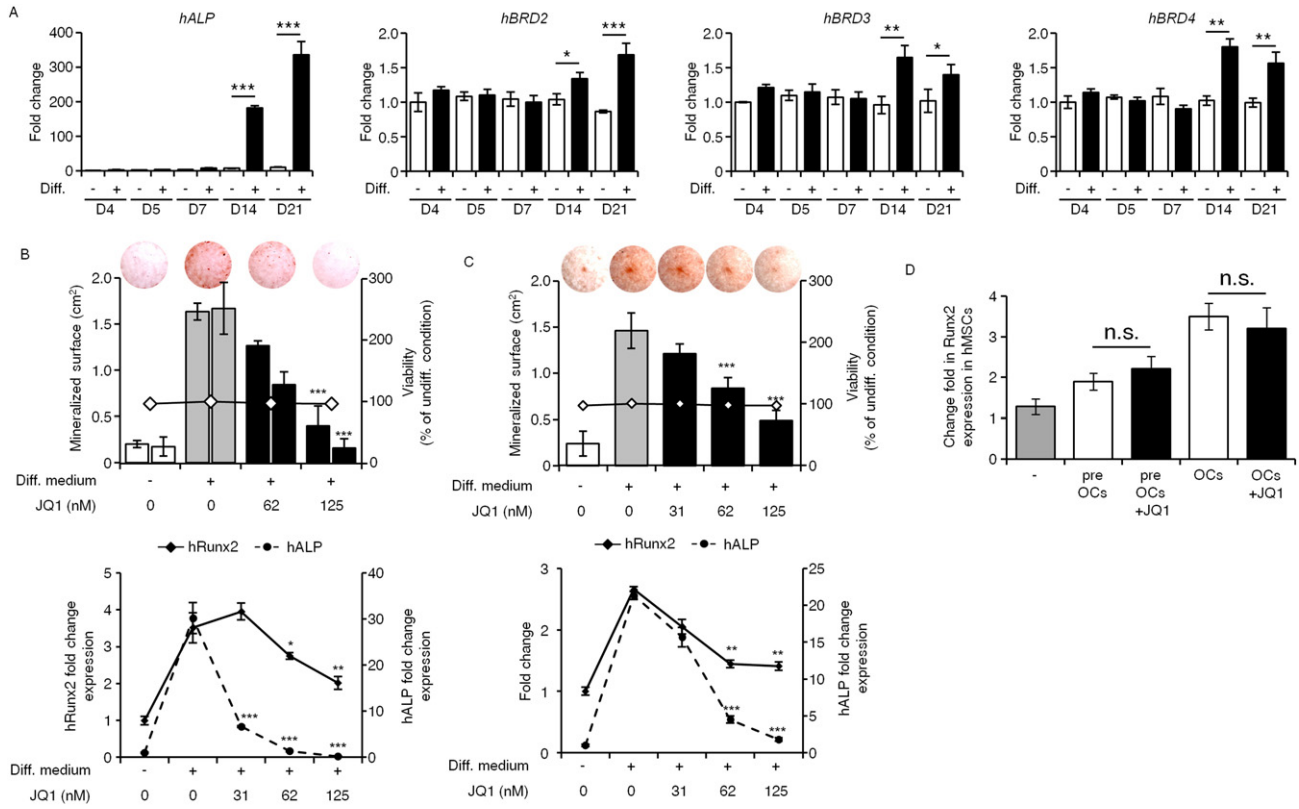

Fig. 4. BET proteins inhibition inhibits osteoblast differentiation. Human MSCs were cultured for 21 days in the presence of OB differentiation medium. (A) mRNA levels of h*ALP*, h*BRD2*, h*BRD3* and h*BRD4* were assessed by qRT-PCR at different time points of the culture (D4, D5, D7, D14 and D21). Results are expressed as fold increase compared to the condition without diff. medium at day 4. (B) hMSCs were cultured for 21 days in the presence of OB differentiation medium and JQ1 for 21 days. Alizarin red staining was performed at the end of the culture and mineralization was quantified (each set of bars represents data from independant donors) and the cell viability was assessed by Crystal Violet (line). mRNA levels of h*Runx2* and h*ALP* were assessed by qRT-PCR. (C) hMSCs were cultured for 21 days in the presence of OB differentiation medium and JQ1 for the last seven days of culture period. Alizarin red Staining was performed at the end of the culture and mineralization was quantified (coloured bars) and the cell viability was assessed by Crystal Violet (line). mRNA levels of h*Runx2* and h*ALP* were assessed by qRT-PCR. (D) Expression of hRunx2 in hMSCs co-cultured with vehicle- or JQ1- treated pre OCs or mature OCs. Error bars show SEM. for $n = 3$ measurement from representative experiments. $^{*}p < 0.05$; $^{*}p < 0.01$; $^{***}p < 0.001$, compared to vehicle by 1-way ANOVA followed by a post test (Bonferroni). (For interpretation of the references to colour in this figure legend, the reader is referred to the web version of this article.)

3.5. Inhibition of BRD2, BRD3 and BRD4 recapitulates JQ1 inhibition of osteoblast differentiation in vitro

To confirm that BET proteins are involved in osteoblast differentiation, human MSCs were cultured in OB differentiation medium and transduced with a combination of shBRD2, shBRD3, shBRD4 (shBRDs). After 3 days, expression of *BRD2*, *BRD3*, and *BRD4* RNA was assessed by qRT-PCR to validate the efficiency of the shRNAs (Fig. 5A). After 21 days of culture, mineralization quantification by alizarin red staining and quantification of *RUNX2* expression revealed a significant inhibition of OB differentiation by shBRDs compared to shLacZ and confirmed that the simultaneous inhibition of the three BRDs recapitulates the effects of JQ1 on OB differentiation (Fig. 5B).

Similarly to the experiments performed on osteoclasts, we asked the question whether BRD2, BRD3 and BRD4 are individually essential for osteoblastogenesis. hMSCs were transduced with shRNAs specific for BRD2, BRD3 or BRD4. Interestingly, silencing of BRD2 or BRD3 reduced the extent of OB differentiation as suggested by a reduction of the mineralized area and h*RUNX2* expression, whereas the transduction of hMSCs with shBRD4 had the opposite effect (Fig. 5C). Indeed, BRD4 knockdown increased the osteoblastic differentiation as revealed by a greater mineralized surface and a stable expression of h*RUNX2* (Fig. 5C).

3.6. BET protein inhibition slightly increases normal bone mass without affecting its mechanical properties

We tested whether BET protein inhibition could affect the normal bone architecture. Healthy 6 week old mice (C57BL6) were treated for 28 days using JQ1 at 50 mg/kg. Von Kossa stained cross sections and μCT images of the metaphyseal region of the tibia revealed an increase in trabecular bone mass (Fig. 6A). JQ1 treatment induced a significant increase in trabecular bone volume (BV/TV, 44%, $p < 0.01$), associated with an increase in trabecular number (Tb.N.) and trabecular thickness

Fig. 5. BET proteins are essential for osteoblast differentiation. (A) Human MSCs were cultured in OB differentiation medium and transduced with a combination of shBRD2, shBRD3, shBRD4 (shBRDs). After 2 days, expression of h*BRD2*, h*BRD3* and h*BRD4* RNA levels were assessed by qRT-PCR (B) After 21 days of culture, mineralization was quantified after staining with alizarin red-S and expression of hRunx2 was assessed by qRT-PCR. (C) Human MSCs were transduced with shBRD2 or shBRD3 or shBRD4. After 2 days, expression of h*BRD2*, h*BRD3* and h*BRD4* RNA level were respectively assessed by qRT-PCR. After 21 days, cultured in OB differentiation medium, mineralization was quantified after staining with alizarin red-S and expression of h*Runx2* expression was assessed by qRT-PCR. Data represent mean ± SEM, $^{*}p < 0.05$; $^{**}p < 0.01$, $^{***}p < 0.001$ compared to control condition by Student *t*-test. The control condition shLacZ is common to the experiments with shBrd2, shBRD3 and shBRD4 in panel C. The same picture has been taken to illustrate the experiments. (For interpretation of the references to colour in this figure legend, the reader is referred to the web version of this article.)

(Tb.Th.) (respectively, 18% $p < 0.01$ and 22% $p < 0.001$; Fig. 6B). A significant increase in cortical bone thickness in the presence of JQ1 was also observed (13.2%, $p < 0.05$; Fig. 6B). The biomechanical properties of the femurs were assessed by three point bending. No changes were observed in terms of bone stiffness and maximum load (Fig. 6C) in the presence of JQ1 treatment, meaning the JQ1 treated bone was as strong

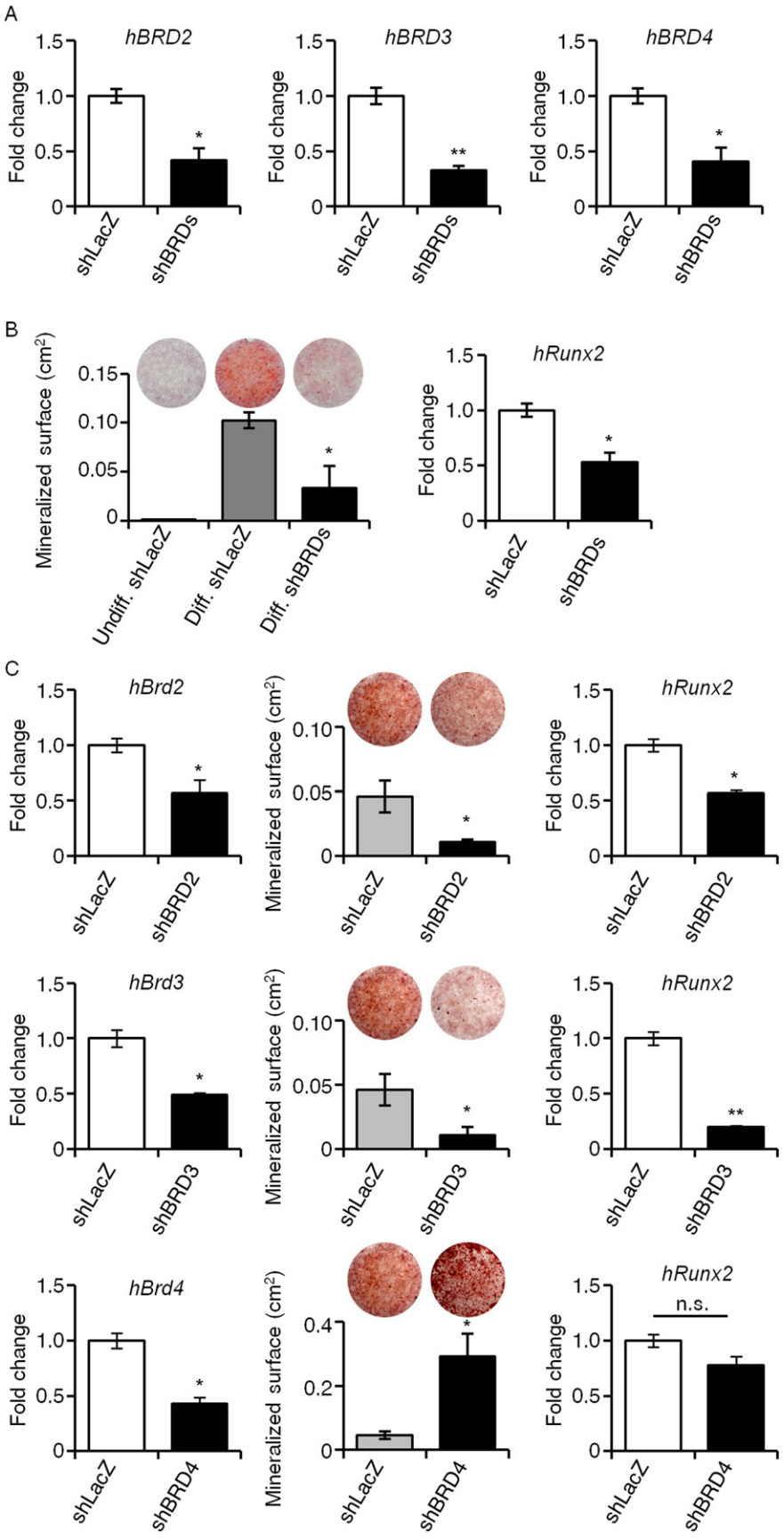

as the vehicle treated bone. Similar results were observed for the analysis of lumbar vertebra L4 (Fig. 6D–E).

3.7. BET protein inhibition decreases osteoclast number in vivo

Histomorphometric analysis of trabecular bone in the proximal tibia showed a significant decrease in osteoclast number in JQ1 treated animals (Oc.N.; Fig. 7A). The number of TRAP-positive OCs lining the bone surface revealed that JQ1 induced an early decrease in osteoclast numbers as early as 3 days after the beginning of treatment which continued to reduce to day 28 (Fig. 7A). Oc.N was significantly decreased at day 7 (37%, $p < 0.05$) compared to vehicle-treated mice. The same serial histological sections were used for Osterix staining revealing the number of osteoblasts lining on bone surface. No significant difference of OB number per millimeter could be observed in presence of JQ1 whatever the time of treatment (Fig. 7B). During the experiment, two injections of fluorescent calcein were performed 7 days and 2 days prior to sacrifice at day 14. On the basis of fluorescence images of the trabecular bone from the tibiae of vehicle or JQ1 treated mice (Fig. 7C), we concluded that JQ1 did not significantly affect the mineral apposition rate (MAR (μm/day)) and bone formation (BFR/BS ($\mu m^2/\mu m^3$/day)) in physiological conditions.

4. Discussion

According to the world health organization, osteoporosis affects >75 million people in the United States, Europe and Japan and the lifetime risk of fracture has been estimated to be between 30 and 40% in developed countries. The treatment of this disease is considered essential to the maintenance of health and quality of life because of its morbid consequences.

Emerging evidences suggest that epigenetic modulations play an important role in bone biology and may offer new targets to treat bone diseases [5,23,24]. Thus, BET proteins are a group of epigenetic regulators that bind to acetylated lysine on histone tails to regulate chromatin accessibility to transcription factors and RNA polymerase [7,8]. Numerous small-molecule were developed to target BET proteins in pre-clinical models of cancers especially in hematological malignancies [9,10,12,25–28]. Currently, some BET protein inhibitors are being tested in early phase clinical trials illustrating the therapeutic potential of this new class of drugs (clinicaltrials.gov references NCT02157636, NCT02259114, NCT02158858 and NCT02308761). In this context, we recently showed that, JQ1, one of the BET protein inhibitor was able to suppress osteosarcoma mediated bone remodeling in a preclinical model [11]. Since then, several studies have shown that BET protein inhibition seems to be a potential candidate for the treatment of bone related diseases associated with inflammation [14–16].

Here we report data to support and confirm that BET protein inhibition could be a promising treatment for osteoporosis. We directly challenged an existing ovariectomy-induced osteopenia and rescued it using JQ1. This preclinical study demonstrates the potential of JQ1 as curative treatment in ovariectomized mice with established bone loss, leading to a greater trabecular bone volume (both in long bones and vertebra) associated with a greater bone strength after only 28 days of treatment. These results corroborate recent studies demonstrating that various BET protein inhibitors could increase bone mass in rheumatoid arthritis, periodontitis and osteoporosis preclinical models [14–16].

Histomorphometric observations revealed a decrease of osteoclast number in OVX-mice at the end of experiment which could be explain by a massive reduction of bone parameters in cancellous bone after 6 weeks of ovariectomy. Nevertheless, histomorphometry revealed an increase of both osteoclast and osteoblast number within the cancellous bone in OVX-animal treated with JQ1 compared to vehicle treated animals. This fact may be explain by our *in vitro* observation showing that BET protein inhibition does not prevent pre OCs and OCs to initiate osteoblastogenesis, suggesting that JQ1 could have a potential anabolic activity. This study over a longer culture period would confirm this observation through quantification of mineralization. We hypothesize that JQ1 can dissociate the two osteoclasts functions and inhibit its bone resorption activity whilst maintaining its osteoblast differentiation activation potential. To demonstrate *in vivo* that JQ1 has anabolic potential in OVX mice, another *in vivo* experiment might be performed using calcein labeling at different time points of the experiment to assess bone formation. This hypothesis is supported by Karsdal et al. who report data supporting the possibility of un-coupling bone resorption and bone formation, with OCs presenting anabolic factors even if their resorption activity is inhibited [29]. Patients suffering from osteopetrosis with mutations in the chloride channel of the osteoclast proton pump are excellent examples of this phenomenon. Indeed, those patients have reduced bone resorption associated with increased bone formation and not the classical secondary decrease in bone formation normally observed with classical anti-resorptive molecules [30]. Moreover, those patients present an increased number of non-resorbing OCs associated with an increased number of active OBs, exactly as we observed after JQ1 treatment [31].

In the present study, we confirmed that intraperitoneal injection of JQ1 did not exert any adverse effect especially on normal bone [15,32]. A moderate increased bone mass was observed without affecting any bone strength parameters. Histomorphological analysis of healthy mice revealed an early decrease in osteoclast numbers without any change in osteoblast number explaining the increase of bone mass. Thus, we could consider that BET protein inhibition has an effect on bone remodeling only in bone disorders such as in osteoporosis.

Mechanistically, our study confirms that BET protein inhibition induces an inhibition of both osteoclast differentiation and activity as well as of osteoblasts *in vitro* [11,25]. Interestingly, we did observe the same effects after BRD2, BRD3 and BRD4 silencing together with shRNAs confirming the central role of the BET proteins in bone cells differentiation and activity. However, the specific BRD4 silencing in human mesenchymal stem cells results in a greater mineralization which could be mediated by BRD2 and BRD3 in substitution for Brd4 and thus regulating genes that are usually activate by BRD4. This hypothesis has to be tested by ChIP for BRD2 and BRD3. The specific silencing of BRD2 and BRD3 caused both disruption of osteoblast and osteoclast differentiation. Thus, considering the higher affinity of JQ1 for BRD4, it appears that BRD4 is the key BET protein targeted by JQ1 in bone biology, exerting specific activity on bone cells. Emerging evidences are considering the activity of BRD4 as a regulator of lineage specific gene associated with enhancer elements [33]. Moreover, aging is widely associated with the accumulation of molecular defects over time and alteration of the normal epigenetic pattern. In this context, it has been suggested that an aging associated disorder such as osteoporosis could have an important epigenetic component [5,34]. Thus, we could consider that in bone related disorders, the activity of BRD4 is modified in bone cells leading to an inhibition of bone formation and activation of bone resorption. JQ1, as a specific inhibitor of BRD4, would blocking these mechanisms, and consequently increase bone mass. It is suggested by Park-Min who showed that BRD4 binds to the promoter of NFATc1, the master transcription factor of osteoclastogenesis, which is displaced with I-BET151 and thus decrease of NFATc1 expression [14]. We did observe similar decrease of NFATc1 expression with JQ1.

In conclusion, BET protein inhibitors result in a decrease in osteoclast differentiation and activity but do not affect their potential to activate osteoblasts. Furthermore, we show that blocking BET protein signaling with JQ1 administration can reverse the bone loss that occurs with estrogen deficiency through increases in bone mass, structure and strength. This robust response suggests that inhibition of BET protein signaling with JQ1 represents a promising new therapeutic approach for the treatment of bone-related disorders.

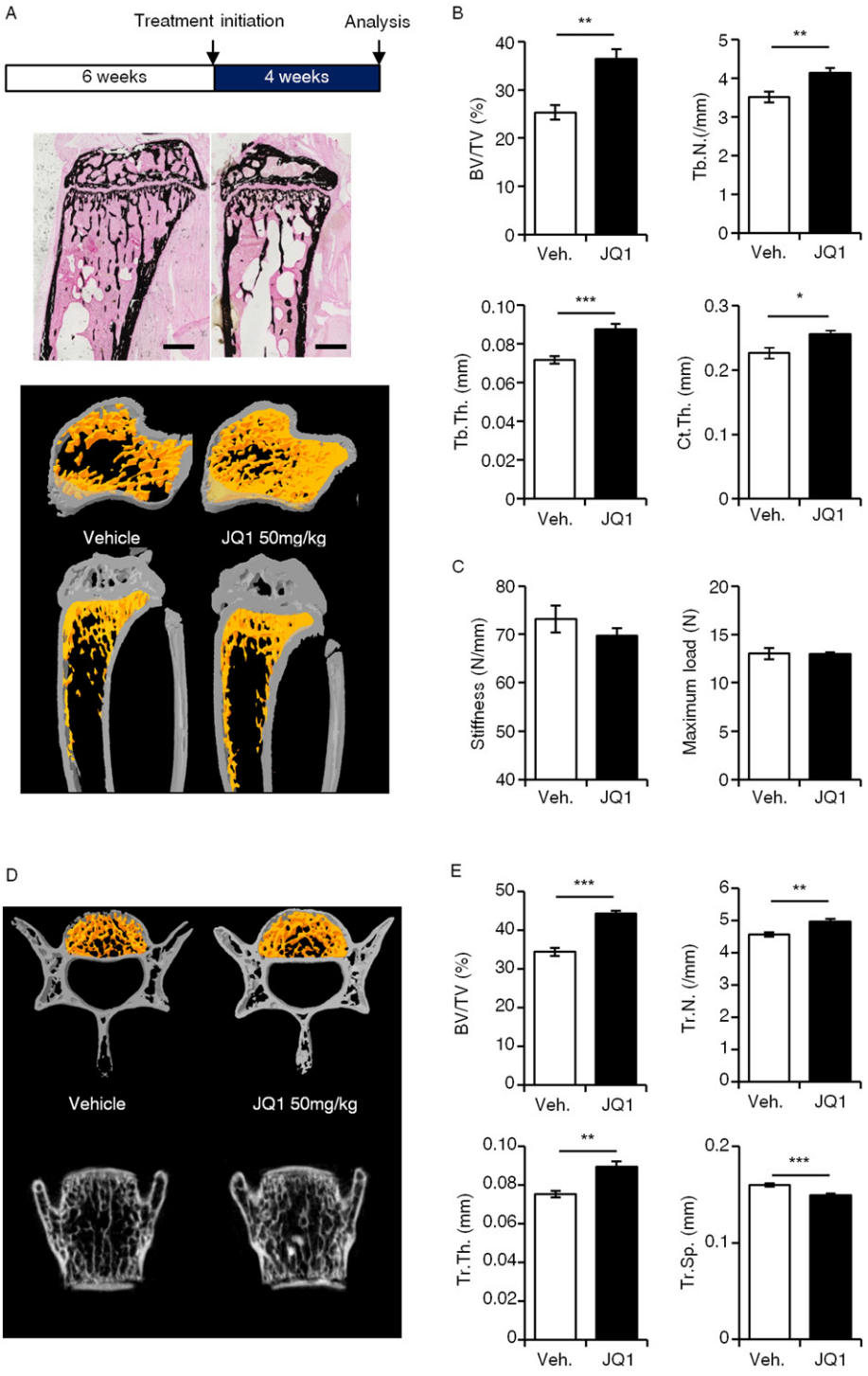

Fig. 6. JQ1 increases normal bone mass without affecting its mechanical properties. (A) Representative longitudinal sections coloured with Von Kossa staining and representative transverse microCT images of the proximal tibia metaphysis, taken *ex vivo*, from mice treated with JQ1 (50 mg/kg) or vehicle (Veh.) for 28 days. (B) MicroCT analysis of trabecular bone volume (BV/TV (%)), trabecular number (Tb.N (/mm), trabecular thickness (Tb.Th (mm)) and cortical thickness (Ct.Th (mm)) of the tibia of mice treated with JQ1 (black bars) or vehicle (open bars) for 28 days ($n = 6$). (C) Three point bending analysis of stiffness and maximum load of the left femur of mice treated with vehicle (open bars) or JQ1 (black bars). ($n = 4$ for each group). (D) Representative longitudinal and transverse microCT images of the lumbar vertebra L4, taken *ex vivo*, from mice treated with JQ1 (50 mg/kg) or vehicle (Veh.) for 28 days. (E) MicroCT analysis of trabecular bone volume (BV/TV (%)), trabecular number (Tb.N (/mm), trabecular thickness (Tb.Th (mm)) and trabecular separation (Tb.Sp (mm)) of the lumbar vertebra L4 of mice treated with JQ1 (black bars) or vehicle (open bars) for 7 days. Data represent mean ± SEM, $^{**}p < 0.01$, $^{***}p < 0.001$ compared to vehicle by Student *t*-test.

Statement of competing financial interest

Dr. Bradner is the scientific founder of Tensha Therapeutics which has licensed drug like inhibitors of BET proteins from the Dana-Farber Cancer Institute for clinical translation as cancer therapeutics.

Author contributions statement

M.B., F.L. and B.O. conceived, designed and performed the research and wrote the manuscript. M.Be., B.B.-L.R., T.Q., C.C. and J.A. performed and analysed experiments. C.J. and L.R.C. contributed to the *in vivo* experiments. R.O. and G.R. performed and analysed the mechanical tests. J.B.

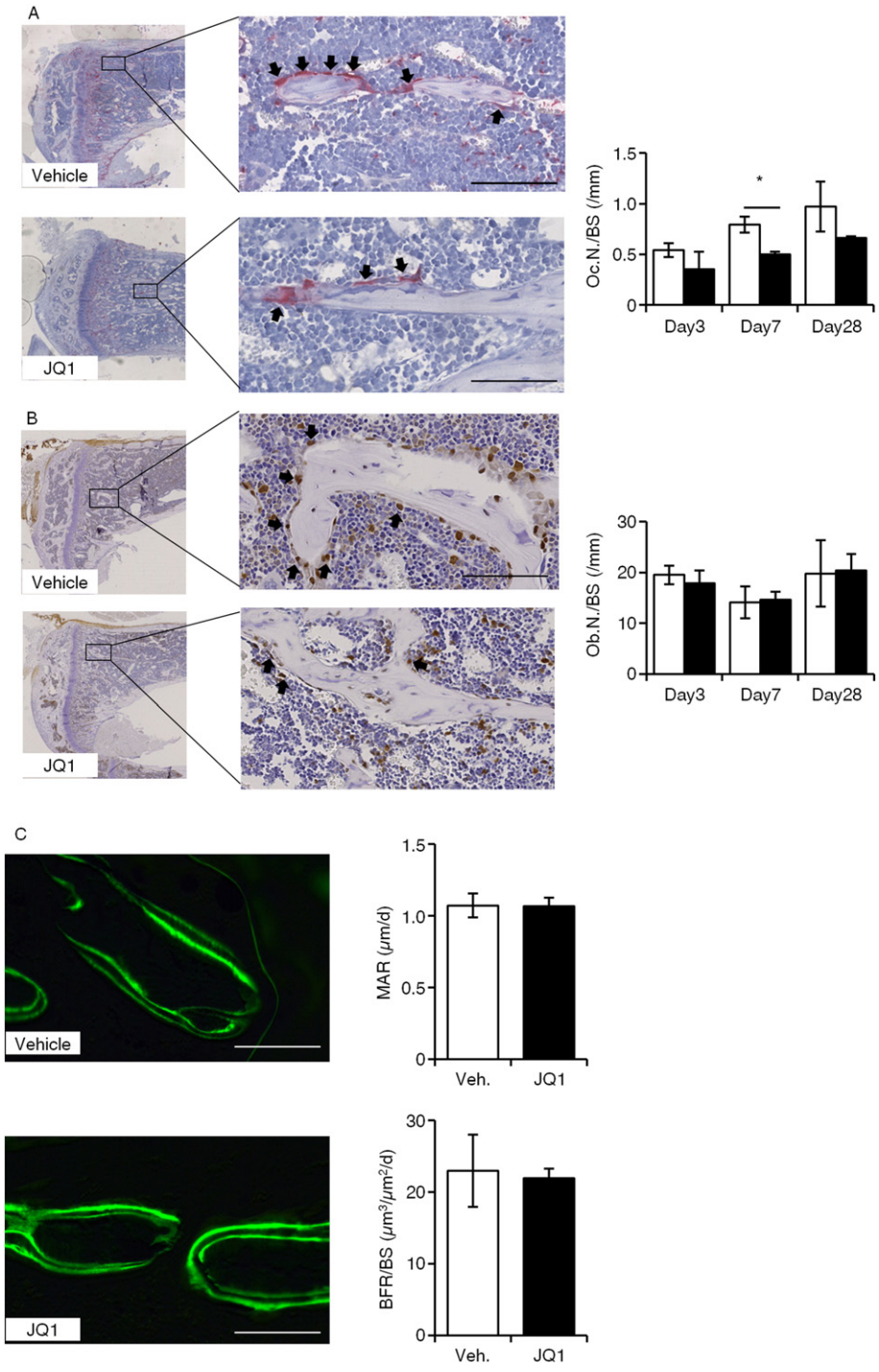

Fig. 7. JQ1 induces an early decrease in osteoclast numbers. (A) Histological sections of the tibiae of mice treated with vehicle or JQ1 at day 7. Arrow identify TRAP-positive osteoclasts lining trabecular bone surfaces. Histogram showing osteoclast number (Oc.N./BS (/mm)) in mice treated with vehicle (open bars) or JQ1 (black bars) for 3 ($n = 6$), 7 ($n = 6$) and 28 days ($n = 6$). (B) Histological sections of the tibiae of mice treated with vehicle or JQ1 at day 7. Arrow identify Osterix-positive osteoblasts lining trabecular bone surfaces. Histogram showing osteoblast number (Ob.N./BS (/mm)) in mice treated with vehicle (open bars) or JQ1 (black bars) for 3 ($n = 6$), 7 ($n = 6$) and 28 days ($n = 6$). (C) Fluorescence images of the tibia of vehicle or JQ1 treated mice. Histograms showing mineral apposition rate (MAR (μm/day)) and bone formation (BFR/BS ($\mu m^2/\mu m^3$/day)) in vehicle (open bars) and JQ1 (black bars) treated mice at day 14. Data represent mean ± SEM. Scale bar 100 μm.

selected and provided JQ1. D.H. provided input into design of JQ1 experiments and manuscript writing. B.O. conceived and oversaw the project.

Acknowledgments

This paper was written as a part of research project which received funding from the Seventh Framework Programme ([FP7/2007–2013]) under grant agreement no. 264817 — BONE-NET.

Camille Jacques is founded by INSERM (Institut National de la Santé et de la Recherche Médicale) and Région Pays de la Loire (grant no. 000381794).

Appendix A. Supplementary data

Supplementary data to this article can be found online at http://dx.doi.org/10.1016/j.bone.2016.09.020.

References

[1] G.A. Rodan, T.J. Martin, Therapeutic approaches to bone diseases, Science 289 (2000) 1508–1514.
[2] M. Baud'huin, L. Duplomb, C. Ruiz Velasco, Y. Fortun, D. Heymann, M. Padrines, Key roles of the OPG-RANK-RANKL system in bone oncology, Expert. Rev. Anticancer. Ther. 7 (2007) 221–232.
[3] M. Baud'huin, N. Solban, M. Cornwall-Brady, D. Sako, Y. Kawamoto, K. Liharska, D. Lath, M.L. Bouxsein, K.W. Underwood, J. Ucran, R. Kumar, E. Pobre, A. Grinberg, J. Seehra, E. Canalis, R.S. Pearsall, P.I. Croucher, A soluble bone morphogenetic protein type IA receptor increases bone mass and bone strength, Proc. Natl. Acad. Sci. U. S. A. 109 (2012) 12207–12212.
[4] M. Zaidi, Skeletal remodeling in health and disease, Nat. Med. 13 (2007) 791–801.
[5] P. Vrtacnik, J. Marc, B. Ostanek, Epigenetic mechanisms in bone, Clin. Chem. Lab. Med. 52 (2014) 589–608.
[6] Y. Liu, X. Zhang, L. Chen, X. Lin, D. Xiong, X. F, Y. LQ, L. EY, Epigenetic mechanisms of bone regeneration and homeostasis, Prog. Biophys. Mol. Biol. (2016).
[7] D.S. Hewings, T.P. Rooney, L.E. Jennings, D. Hay, S. CJ, B. PE, S. Knapp, C. SJ, Progress in the development and application of small molecule inhibitors of bromodomain-acetyl-lysine interactions, J. Med. Chem. (2012).
[8] R.K. Prinjha, J. Witherington, K. Lee, Place your BETs: the therapeutic potential of bromodomains, Trends Pharmacol. Sci. 33 (2012) 146–153.
[9] M.A. Dawson, R.K. Prinjha, A. Dittmann, G. Giotopoulos, M. Bantscheff, W.I. Chan, S.C. Robson, C.W. Chung, C. Hopf, M.M. Savitski, C. Huthmacher, E. Gudgin, D. Lugo, S. Beinke, T.D. Chapman, E.J. Roberts, P.E. Soden, K.R. Auger, O. Mirguet, K. Doehner, R. Delwel, A.K. Burnett, P. Jeffrey, G. Drewes, K. Lee, B.J. Huntly, T. Kouzarides, Inhibition of BET recruitment to chromatin as an effective treatment for MLL-fusion leukaemia, Nature 478 (2011) 529–533.
[10] P. Filippakopoulos, J. Qi, S. Picaud, Y. Shen, W.B. Smith, O. Fedorov, E.M. Morse, T. Keates, T.T. Hickman, I. Felletar, M. Philpott, S. Munro, M.R. McKeown, Y. Wang, A.L. Christie, N. West, M.J. Cameron, B. Schwartz, T.D. Heightman, N. La Thangue, C.A. French, O. Wiest, A.L. Kung, S. Knapp, J.E. Bradner, Selective inhibition of BET bromodomains, Nature 468 (2010) 1067–1073.
[11] F. Lamoureux, M. Baud'huin, L. Rodriguez Calleja, C. Jacques, M. Berreur, F. Redini, F. Lecanda, J.E. Bradner, D. Heymann, B. Ory, Selective inhibition of BET bromodomain epigenetic signalling interferes with the bone-associated tumour vicious cycle, Nat. Commun. 5 (2014) 3511.
[12] J. Zuber, J. Shi, E. Wang, A.R. Rappaport, H. Herrmann, E.A. Sison, D. Magoon, J. Qi, K. Blatt, M. Wunderlich, M.J. Taylor, C. Johns, A. Chicas, J.C. Mulloy, S.C. Kogan, P. Brown, P. Valent, J.E. Bradner, S.W. Lowe, C.R. Vakoc, RNAi screen identifies Brd4 as a therapeutic target in acute myeloid leukaemia, Nature 478 (2011) 524–528.
[13] I.A. Asangani, V.L. Dommeti, X. Wang, R. Malik, M. Cieslik, R. Yang, J. Escara-Wilke, K. Wilder-Romans, S. Dhanireddy, C. Engelke, M.K. Iyer, X. Jing, Y.M. Wu, X. Cao, Z.S. Qin, S. Wang, F.Y. Feng, A.M. Chinnaiyan, Therapeutic targeting of BET bromodomain proteins in castration-resistant prostate cancer, Nature 510 (2014) 278–282.
[14] K.H. Park-Min, E. Lim, M.J. Lee, S.H. Park, E. Giannopoulou, A. Yarilina, M. van der Meulen, B. Zhao, N. Smithers, J. Witherington, K. Lee, P.P. Tak, R.K. Prinjha, L.B. Ivashkiv, Inhibition of osteoclastogenesis and inflammatory bone resorption by targeting BET proteins and epigenetic regulation, Nat. Commun. 5 (2014) 5418.
[15] S. Meng, L. Zhang, Y. Tang, Q. Tu, L. Zheng, L. Yu, D. Murray, J. Cheng, S.H. Kim, X. Zhou, J. Chen, BET inhibitor JQ1 blocks inflammation and bone destruction, J. Dent. Res. 93 (2014) 657–662.
[16] B. Gjoksi, C. Ghayor, B. Siegenthaler, N. Ruangsawasdi, M. Zenobi-Wong, F.E. Weber, The epigenetically active small chemical *N*-methyl pyrrolidone (NMP) prevents estrogen depletion induced osteoporosis, Bone 78 (2015) 114–121.
[17] B. Brounais, C. Chipoy, K. Mori, C. Charrier, S. Battaglia, P. Pilet, C.D. Richards, D. Heymann, F. Redini, F. Blanchard, Oncostatin M induces bone loss and sensitizes rat osteosarcoma to the antitumor effect of Midostaurin in vivo, Clin. Cancer Res. 14 (2008) 5400–5409.
[18] B. Gobin, M.B. Huin, F. Lamoureux, B. Ory, C. Charrier, R. Lanel, S. Battaglia, F. Redini, F. Lezot, F. Blanchard, D. Heymann, BYL719, a new alpha-specific PI3K inhibitor: single administration and in combination with conventional chemotherapy for the treatment of osteosarcoma, Int. J. Cancer 136 (2015) 784–796.
[19] L. Duplomb, M. Baud'huin, C. Charrier, M. Berreur, V. Trichet, F. Blanchard, D. Heymann, Interleukin-6 inhibits receptor activator of nuclear factor kappaB ligand-induced osteoclastogenesis by diverting cells into the macrophage lineage: key role of Serine727 phosphorylation of signal transducer and activator of transcription 3, Endocrinology 149 (2008) 3688–3697.
[20] C. Chipoy, M. Berreur, S. Couillaud, G. Pradal, F. Vallette, C. Colombeix, F. Redini, D. Heymann, F. Blanchard, Downregulation of osteoblast markers and induction of the glial fibrillary acidic protein by oncostatin M in osteosarcoma cells require PKCdelta and STAT3, J. Bone Miner. Res. 19 (2004) 1850–1861.
[21] V. Trichet, C. Benezech, C. Dousset, M.C. Gesnel, M. Bonneville, R. Breathnach, Complex interplay of activating and inhibitory signals received by Vgamma9Vdelta2 T cells revealed by target cell beta2-microglobulin knockdown, J. Immunol. 177 (2006) 6129–6136.
[22] H. Takayanagi, The role of NFAT in osteoclast formation, Ann. N. Y. Acad. Sci. 1116 (2007) 227–237.
[23] L.B. Ivashkiv, Metabolic-epigenetic coupling in osteoclast differentiation, Nat. Med. 21 (2015) 212–213.
[24] T. Yasui, J. Hirose, H. Aburatani, S. Tanaka, Epigenetic regulation of osteoclast differentiation, Ann. N. Y. Acad. Sci. 1240 (2011) 7–13.
[25] A. Chaidos, V. Caputo, A. Karadimitris, Inhibition of bromodomain and extra-terminal proteins (BET) as a potential therapeutic approach in haematological malignancies: emerging preclinical and clinical evidence, Ther. Adv. Hematol. 6 (2015) 128–141.
[26] J.A. Mertz, A.R. Conery, B.M. Bryant, P. Sandy, S. Balasubramanian, D.A. Mele, L. Bergeron, S. RJ 3rd., Targeting MYC dependence in cancer by inhibiting BET bromodomains, Proc. Natl. Acad. Sci. U. S. A. 108 (2011) 16669–16674.
[27] J.E. Delmore, G.C. Issa, M.E. Lemieux, P.B. Rahl, J. Shi, H.M. Jacobs, E. Kastritis, T. Gilpatrick, R.M. Paranal, J. Qi, M. Chesi, A.C. Schinzel, M.R. McKeown, T.P. Heffernan, C.R. Vakoc, P.L. Bergsagel, I.M. Ghobrial, P.G. Richardson, R.A. Young, W.C. Hahn, K.C. Anderson, A.L. Kung, J.E. Bradner, C.S. Mitsiades, BET bromodomain inhibition as a therapeutic strategy to target c-Myc, Cell 146 (2011) 904–917.
[28] C.J. Ott, N. Kopp, L. Bird, R.M. Paranal, J. Qi, T. Bowman, S.J. Rodig, A.L. Kung, J.E. Bradner, D.M. Weinstock, BET bromodomain inhibition targets both c-MYC and IL7R in high-risk acute lymphoblastic leukemia, Blood (2012).
[29] M.A. Karsdal, T.J. Martin, J. Bollerslev, C. Christiansen, K. Henriksen, Are nonresorbing osteoclasts sources of bone anabolic activity? J. Bone Miner. Res. 22 (2007) 487–494.
[30] J. Bollerslev, T. Steiniche, F. Melsen, L. Mosekilde, Structural and histomorphometric studies of iliac crest trabecular and cortical bone in autosomal dominant osteopetrosis: a study of two radiological types, Bone 10 (1989) 19–24.
[31] J. Bollerslev, S.C. Marks Jr., S. Pockwinse, M. Kassem, K. Brixen, T. Steiniche, L. Mosekilde, Ultrastructural investigations of bone resorptive cells in two types of autosomal dominant osteopetrosis, Bone 14 (1993) 865–869.
[32] M.M. Matzuk, M.R. McKeown, P. Filippakopoulos, Q. Li, L. Ma, J.E. Agno, M.E. Lemieux, S. Picaud, R.N. Yu, J. Qi, S. Knapp, J.E. Bradner, Small-molecule inhibition of BRDT for male contraception, Cell 150 (2012) 673–684.
[33] J. Shi, C.R. Vakoc, The mechanisms behind the therapeutic activity of BET bromodomain inhibition, Mol. Cell 54 (2014) 728–736.
[34] P.J. Marie, Bone cell senescence: mechanisms and perspectives, J. Bone Miner. Res. 29 (2014) 1311–1321.